Letter

Fundamental Limits of Doppler Shift-Based, ToA-Based, and TDoA-Based Underwater Localization

Zijun Gong, *Member, IEEE*, Cheng Li, *Senior Member, IEEE*, and Ruoyu Su, *Member, IEEE*

Dear Editor,

This paper is concerned with the underwater localization based on acoustic signals. Specifically, we will focus on the search of an underwater target that can constantly broadcast a beacon signal, such as a black box. Common measurements for localization are Doppler shift [1], time of arrival (ToA) [2]–[4], time difference of arrival (TDoA) [5], [6], angle of arrival (AoA) [7], etc. In this paper we will investigate the fundamental limits of Doppler shift-Based, ToA-Based, TDoA-based underwater localization. Note that AoA is not covered, because Doppler shift can be viewed as one type of AoA. The discussion will focus on short-baseline positioning with a mobile anchor, i.e., an autonomous underwater vehicle (AUV). Due to the large distance and the limited battery life of the AUV, the target is quite likely to lie outside the convex hull of the AUV's trajectory. In such cases, we will show that accurate localization is almost impossible by exclusively dependent on a single type of measurements. However, system performance will be significantly improved by combing Doppler shift with ToA or TDoA measurements. The reason for such improvement will be unveiled theoretically and numerically in this letter.

Related Work: In underwater localization, information fusion is an important topic. For example, the authors of [7] combined ToA and AoA for object localization through the Bayesian method. In [8]–[10], the authors discussed the possibility of employing both ToA and Doppler shift for localization. Most related work focuses on static targets, while the mobility can be easily accommodated by jointly estimating the position and velocity [9], [11]. In [12], the authors showed that cooperative localization of a group of AUVs is possible, even without anchors in the network.

In this letter, we will investigate the underwater target localization based on a mobile anchor, i.e., AUV [13]. The target is constantly broadcasting a probe signal, and the AUV can receive the beacon signal and extract various position-related measurements for localization. It is well known that the positioning error will be very large when the mobile anchor is far away from the target, due to the huge geometric dilution of precision (GDOP), which amplifies the measurement noise. This will hold true if we conduct localization exclusively depending on one type of measurements. In this paper, we will formulate and explain this issue mathematically, and show that by using diverse measurements, such as Doppler shift with ToA or TDoA, this problem can be resolved.

Our contribution in this paper lies in the following aspects.

1) We derived the Cramér-Rao lower bound (CRLB) of positioning error for Doppler shift-Based, ToA-Based and TDoA-based systems.

2) We unveiled two fundamental reasons for the boost of GDOP when the AUV is far away from the target: the huge condition number of the covariance matrix and the large distance.

3) We mathematically and geometrically explained that by combining Doppler shift with ToA or TDoA, the positioning error can be significantly reduced.

Doppler-based localization: Suppose the target is located at $\mathbf{x}$. The AUV is initially located at $\mathbf{x}_a$ and moves at a velocity of $\mathbf{v}$. Without loss of generality, suppose the target is stationary, and the radial velocity of the AUV with respect to the target will be

$$v_r = (\mathbf{x}_a - \mathbf{x})^T \mathbf{v}/\|\mathbf{x}_a - \mathbf{x}\|. \tag{1}$$

A negative v_r means the T-R (Transmitter-Receiver) distance is decreasing, while a positive v_r means the opposite. The target broadcasts a tone at f_0 Hz, and the received baseband signal at the AUV will have a different frequency due to the Doppler effect. Define the scaling factor as $\rho = 1 - v_r/c$, with c being the underwater acoustic speed, and the Doppler shift will be

$$f_D = f_0(\rho - 1) = -f_0 v_r/c. \tag{2}$$

With the AUV's position and velocity known, the Doppler shift measurements are dependent on the target's position. To quantify how strong the relation is, we can derive the gradient as

$$\nabla_{\mathbf{x}} f_D = -\frac{f_0}{c}\frac{\partial v_r}{\partial \mathbf{x}} = \frac{f_0}{cd} \times (\mathbf{v} - (\mathbf{x}_a - \mathbf{x})v_r/d) \tag{3}$$

with $d = \|\mathbf{x}_a - \mathbf{x}\|$ denoting the distance between the AUV and the target. Define $\mathbf{a} = (\mathbf{x}_a - \mathbf{x})/d$, and we have $(\mathbf{x}_a - \mathbf{x})v_r/d = v_r\mathbf{a}$, which is the 2D radial velocity of the AUV with respect to the target, as shown in Fig. 1. The tangential velocity follows as:

$$\mathbf{v}_t = \mathbf{v} - v_r\mathbf{a} = \mathbf{v} - \mathbf{a}\mathbf{a}^T\mathbf{v} = (\mathbf{I} - \mathbf{a}\mathbf{a}^T)\mathbf{v} \tag{4}$$

where we implicitly used the fact $v_r = \mathbf{a}^T\mathbf{v}$. The gradient can then be rewritten in a simplified form as

$$\nabla_{\mathbf{x}} f_D = \frac{f_0}{cd} \times \mathbf{v}_t. \tag{5}$$

When the AUV moves around, we can take the Doppler shift measurements at different locations, i.e., the AUV is located at $\mathbf{x}_m$ for the m-th Doppler shift measurement $f_D^{(m)}$. The real-time distance is $d_m = \|\mathbf{x} - \mathbf{x}_m\|$. In this case, the tangential velocity is given as

$$\mathbf{v}_{t,m} = \underbrace{(\mathbf{I} - \mathbf{a}_m\mathbf{a}_m^T)}_{\mathbf{A}_m}\mathbf{v}_m \tag{6}$$

with $\mathbf{v}_m$ being the velocity and $\mathbf{a}_m = (\mathbf{x}_m - \mathbf{x})/d_m$.

Without loss of generality, we assume the estimation error of the Doppler shift follows zero-mean Gaussian distribution, with a variance of σ_f^2. Thus, the fisher information matrix (FIM) concerning $\mathbf{x}$ will be

$$\mathbf{F}_{\mathbf{x}} = \frac{1}{\sigma_f^2}\sum_{m=0}^{M-1} \nabla_{\mathbf{x}} f_D^{(m)} \nabla_{\mathbf{x}}^T f_D^{(m)} = \frac{f_0^2}{c^2\sigma_f^2}\sum_{m=0}^{M-1}\frac{\mathbf{v}_{t,m}\mathbf{v}_{t,m}^T}{d_m^2} \tag{7}$$

with M being the total number of measurements. Define the geometric centre of $\mathbf{x}_m$'s as $\bar{\mathbf{x}} = \frac{1}{M}\sum_m \mathbf{x}_m$, and $\bar{d} = \|\bar{\mathbf{x}} - \mathbf{x}\|$, leading to $\bar{d} \approx d_m$ in the far field. The CRLB of positioning error is approximately

$$\mathbf{R}_{\mathbf{x}} = \sigma_f^2\bar{d}^2\lambda_0^2\left(\sum_m \mathbf{v}_{t,m}\mathbf{v}_{t,m}^T\right)^{-1} \tag{8}$$

with $\lambda_0 = c/f_0$. When the AUV is very far away from the target, accurate localization becomes impossible for two reasons. First, because $\mathbf{A}_m \approx \mathbf{A}_{m'}$ (see definition in (6)), the rank of $\mathbf{R}_{\mathbf{x}}$ will be almost equal to one (for 3D scenarios, the rank will be almost equal to two, still rank-deficient). As a result, the covariance matrix will have a very large eigenvalue, leading to huge positioning error. Second, the positioning error is proportional to the distance between the AUV and the target, as we can see in (8).

ToA-based and TDoA-based localization: As we can see, the Doppler-based localization techniques have poor performance in the far field. In this section, we investigate another two alternatives, the ToA- and TDoA-based approaches. Suppose the AUV is located at $\mathbf{x}_m$ for the m-th measurement and the corresponding propagation delay will be $\tau_m = d_m/c$, estimated as $\hat{\tau}_m$. Consider i.i.d. zero-mean Gaussian noise in ToA measurements, with a variance of σ_t^2. The FIM of positioning error can then be derived as

Corresponding author: Zijun Gong.

Citation: Z. J. Gong, C. Li, and R. Y. Su, "Fundamental limits of doppler shift-based, ToA-based, and TDoA-based underwater localization," *IEEE/CAA J. Autom. Sinica*, vol. 10, no. 7, pp. 1637–1639, Jul. 2023.

Z. J. Gong is with the Hong Kong University of Science and Technology (Guangzhou), IOT Thrust, Guangzhou 511400, and also with the Department of Electronic and Computer Engineering, The Hong Kong University of Science and Technology, Hong Kong 999077, China (e-mail: gongzijun@ust.hk).

C. Li is with the Faculty of Engineering and Applied Science, Memorial University of Newfoundland, Newfoundland A1B 3X5, Canada (e-mail: licheng@mun.ca).

R. Y. Su is with the School of Internet of Things, Nanjing University of Posts and Telecommunications, Nanjing 210003, China (e-mail: suruoyu@njupt.edu.cn).

Color versions of one or more of the figures in this paper are available online at http://ieeexplore.ieee.org.

Digital Object Identifier 10.1109/JAS.2023.123282

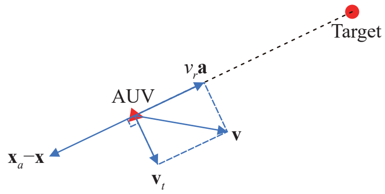

Fig. 1. Illustration of Doppler shift-based positioning.

$$\mathbf{F}_{\mathbf{x}}=\frac{1}{\sigma_t^2}\sum_m \nabla_{\mathbf{x}}\tau_m\nabla_{\mathbf{x}}^T\tau_m=\frac{1}{c^2\sigma_t^2}\sum_m \mathbf{a}_m\mathbf{a}_m^T.$$

In the far field, similar to the Doppler-based case, the FIM (or covariance matrix, equivalently) has huge condition number, leading to terrible GDOP and very low positioning accuracy.

For the TDoA-based case, there is an unknown time difference between the Tx and Rx, i.e., Δt. Therefore, there will be an extra parameter to estimate, i.e., $\boldsymbol{\theta}=[\mathbf{x}^T,\Delta t]^T$. In this case, τ_m is related to not only the position but also the time difference, i.e., $\tau_m=\|\mathbf{x}-\mathbf{x}_m\|/c+\Delta t$. Define $\boldsymbol{\tau}$ as $\boldsymbol{\tau}=[\tau_0,\tau_1,\ldots,\tau_{M-1}]^T$, and the Jacobian is given as

$$\nabla_{\boldsymbol{\theta}}\boldsymbol{\tau}=\frac{1}{c}\left[\mathbf{A}^T,c\mathbf{1}_M\right] \tag{9}$$

where $\mathbf{A}=[\mathbf{a}_0,\mathbf{a}_1,\ldots,\mathbf{a}_{M-1}]$ and $\mathbf{1}_M\in\mathbb{R}^M$ is a vector of ones. Then, the FIM concerning $\boldsymbol{\theta}$ will be

$$\mathbf{F}_{\boldsymbol{\theta}}=\frac{1}{\sigma_t^2}\nabla_{\boldsymbol{\theta}}^T\boldsymbol{\tau}\nabla_{\boldsymbol{\theta}}\boldsymbol{\tau}=\frac{1}{c^2\sigma_t^2}\begin{bmatrix}\mathbf{A}\mathbf{A}^T & c\mathbf{A}\mathbf{1}_M\\ c\mathbf{A}\mathbf{1}_M & Mc^2\end{bmatrix}. \tag{10}$$

The CRLB of positioning error will be

$$\mathbf{R}_{\mathbf{x}}=\mathbf{F}_{\boldsymbol{\theta}}^{-1}[1:2,1:2]=\frac{1}{c^2\sigma_t^2}\left(\mathbf{A}\mathbf{A}^T-M\bar{\mathbf{a}}\bar{\mathbf{a}}^T\right)^{-1} \tag{11}$$

with $\bar{\mathbf{a}}=\frac{1}{M}\sum_m\mathbf{a}_m$, i.e., the unit vector pointing from the target to the geometric centre of $\mathbf{x}_m$'s. Note that we can rewrite the CRLB as

$$\mathbf{R}_{\mathbf{x}}=\frac{1}{c^2\sigma_t^2}\left(\sum_m(\mathbf{a}_m-\bar{\mathbf{a}})(\mathbf{a}_m-\bar{\mathbf{a}})^T\right)^{-1}. \tag{12}$$

In the far field, we have $d_m\approx d_{m'}$, leading to

$$\mathbf{a}_m-\mathbf{a}=\frac{\mathbf{x}_m-\mathbf{x}}{\|\mathbf{x}_m-\mathbf{x}\|}-\frac{\bar{\mathbf{x}}-\mathbf{x}}{\|\bar{\mathbf{x}}-\mathbf{x}\|}\approx(\mathbf{x}_m-\bar{\mathbf{x}})/\bar{d}. \tag{13}$$

Similar to the Doppler-based case, the positioning error of the TDoA-based method is also proportional to the distance, i.e., $\bar{d}$.

As we can see, it is very difficult to get accurate localization result exclusively depending on Doppler shift, ToA, or TDoA measurements. However, a very interesting observation is that the subspace spanned by the FIM of the ToA-based case is almost orthogonal to that of the Doppler shift-based case. That is to say, ToA and Doppler shift measurements are complementary in the far field. Mathematically, $\mathbf{v}_{t,m}$ and $\mathbf{a}_m$ are orthogonal for any m, and they construct the sub-spaces of the covariance matrix of Doppler shift-based and ToA-based positioning errors, respectively. As a result, by combining them together, we can significantly improve the accuracy! This is clearly visualized in Fig. 2.

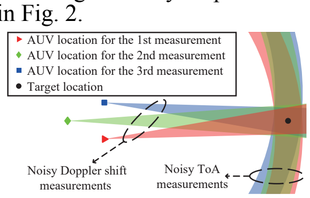

Fig. 2. ToA-based and Doppler-based localization.

As we can see, the AUV keeps moving around and takes ToA and Doppler shift measurements at three different positions. Due to noise, these measurements are not absolutely accurate. When we exclusively conduct localization based on ranging, with each ToA measurement we can get a belt, where the target lies. The width of the belt is dependent on ToA measurement error. For each Doppler shift measurement we get a triangle, the width of which is dependent on frequency measurement error. When the AUV is far away from the target, the area of uncertainty will be very large if we exclusively depend on one type of measurement for localization. Specifically, for the ToA-based case, we can see that three belts almost overlap. For the case of Doppler shift-based localization, we will have three overlapped triangles. Mathematically, this results from the rank-deficient FIM (or covariance matrix) in (8) and (12). However, if we combine the ToA and Doppler shift measurements, the uncertainty (or overlapping area) will be dramatically reduced. This comes from the power of measurement diversity and complementarity. Therefore, the next question is how can we simultaneously get Doppler shift measurements and ToA or TDoA. One option is to use the linear frequency modulated (LFM) signals for probing.

Localization based on LFM signals: Consider an AUV moving around and a target periodically broadcasting a LFM signal

$$s(t)=Ae^{j(2\pi f_0t+k\pi t^2+\phi)},\quad (t\in[0,T]). \tag{14}$$

The total bandwidth is $B=kT$. Consider a time scaling factor of ρ and a propagation delay of τ at $t=0$, the received signal will be

$$r(t)=s(\rho(t-\tau))+w(t) \tag{15}$$

where $w(t)$ is additive white Gaussian noise. Apparently, the received signal is another LFM signal with different initial frequency and frequency rate. Specifically, we have

$$r(t)=\tilde{A}\exp\left[j\left(2\pi\tilde{f}_0t+\tilde{k}t^2+\tilde{\phi}\right)\right]+w(t) \tag{16}$$

with $\tilde{A}$ being the amplitude and other parameters given by

$$\tilde{f}_0=f_0\rho-k\rho^2\tau,\ \tilde{k}=k\rho^2,\ \tilde{\phi}=k\rho^2\tau^2-2f_0\rho\tau+\phi$$

Suppose the sampling frequency is f_s, corresponding to a sampling period $T_s=1/f_s$, and the sampled sequence will be

$$\mathbf{r}[n]=r(nT_s)=\tilde{A}e^{j(n2\pi\tilde{f}_0T_s+\tilde{k}\pi T_s^2n^2+\tilde{\phi})}+\mathbf{w}[n] \tag{17}$$

where $\mathbf{w}[n]$ is additive white Gaussian noise, i.e., $\mathbf{w}\sim\mathcal{CN}(\mathbf{0},\sigma^2\mathbf{I})$ with σ^2 denoting the variance of measurement noise. Consider $\boldsymbol{\mu}=[\tilde{f}_0,\tilde{k},\tilde{\phi},\tilde{A}]^T$, and N is the total number of samples. For $N>>1$, we have the following asymptotic result: $\sum_n n^L\sim N^{L+1}/(L+1)$, leading to the asymptotic FIM as:

$$\mathbf{F}_{\boldsymbol{\mu}}\sim\frac{2N\tilde{A}^2}{\sigma^2}\begin{bmatrix}4\pi^2T^2/3 & \pi^2T^3/2 & \pi T & 0\\ \pi^2T^3/2 & \pi^2T^4/5 & \pi T^2/3 & 0\\ \pi T & \pi T^2/3 & 1 & 0\\ 0 & 0 & 0 & 1/\tilde{A}^2\end{bmatrix}$$

with $T=NT_s$, the total sampling time. For notational conciseness, we define $\mathbf{A}$ and $\mathbf{b}$ as

$$\mathbf{A}=\begin{bmatrix}4\pi^2T^2/3 & \pi^2T^3/2\\ \pi^2T^3/2 & \pi^2T^4/5\end{bmatrix},\ \mathbf{b}=\begin{bmatrix}\pi T\\ \pi T^2/3\end{bmatrix}. \tag{18}$$

Since we are only interested in position-related parameters, i.e., $\tilde{f}_0$ and $\tilde{k}_0$, it is natural to define $\boldsymbol{\phi}=[\tilde{f}_0,\tilde{k}_0]^T$, and the corresponding CRLB concerning $\boldsymbol{\phi}$ is

$$\begin{aligned}\mathbf{R}_{\boldsymbol{\phi}}&=\mathbf{F}_{\boldsymbol{\mu}}^{-1}[1:2,1:2]=\frac{\sigma^2}{2N\tilde{A}^2}\left(\mathbf{A}-\mathbf{b}\mathbf{b}^T\right)^{-1}\\ &=\frac{\sigma^2}{N\tilde{A}^2}\times\frac{3}{\pi^2T^2}\begin{bmatrix}8 & -15/T\\ -15/T & 30/T^2\end{bmatrix}.\end{aligned} \tag{19}$$

From the results, we can see that the estimation error of $\tilde{f}_0$ is inversely proportional to T, while that of $\tilde{k}$ is inversely proportional to T^2.

CRLB of positioning error with LFM signals: For localization, we need to take multiple measurements. Suppose the received signal of the m-th measurement has an amplitude of $\tilde{A}_m$, with initial frequency and frequency rate equal to $\tilde{f}_m$ and $\tilde{k}_m$, respectively. After estimating $\tilde{f}_m$ and $\tilde{k}_m$, we can compute the corresponding time scaling factor and propagation delay, i.e., ρ_m and τ_m. For notation convenience, we define $\boldsymbol{\phi}_m=[\tilde{f}_m,\tilde{k}_m]^T$ and $\boldsymbol{\eta}_m=[\rho_m,\tau_m]^T$. Suppose the CRLB of $\boldsymbol{\phi}_m$ is $\mathbf{R}_{\boldsymbol{\phi}_m}$, and the CRLB of $\boldsymbol{\eta}_m$ will then be

$$\mathbf{F}_{\boldsymbol{\eta}_m}=\nabla_{\boldsymbol{\eta}_m}^T\boldsymbol{\phi}_m\mathbf{R}_{\boldsymbol{\phi}_m}^{-1}\nabla_{\boldsymbol{\eta}_m}\boldsymbol{\phi}_m \tag{20}$$

with the Jacobian given as

$$\nabla_{\boldsymbol{\eta}_m}\boldsymbol{\phi}_m=\begin{bmatrix}f_0-2k\rho_m\tau_m & -k\rho_m^2\\ 2k\rho_m & 0\end{bmatrix}. \tag{21}$$

With the estimated τ_m's and ρ_m's, we can then localize the target. Consider 2D localization, and suppose the target is located at $\mathbf{x}$. The FIM concerning $\mathbf{x}$ is

$$\mathbf{F}_{\mathbf{x}}=\sum_m\nabla_{\mathbf{x}}^T\boldsymbol{\eta}_m\mathbf{F}_{\boldsymbol{\eta}_m}\nabla_{\mathbf{x}}\boldsymbol{\eta}_m \tag{22}$$

and the Jacobian is given as

$$\mathbf{P}_m = \frac{1}{c}\left[\mathbf{v}_{t,m}/d_m, -\mathbf{a}_m\right]^T. \tag{23}$$

The CRLB of positioning error will be

$$\mathbf{R}_\mathbf{x} = \left(\sum_m \mathbf{P}_m^T \mathbf{F}_{\boldsymbol{\eta}_m} \mathbf{P}_m\right)^{-1}. \tag{24}$$

Similar to the TDoA-based approach, when the ToA cannot be directly measured, we can still localize the target by introducing an extra unknown, i.e., the clock bias Δt. Specifically, we define $\boldsymbol{\theta} = [\mathbf{x}^T, \Delta t]^T$, and the Jacobian of $\boldsymbol{\eta}_m$ with respect to $\boldsymbol{\theta}$ is

$$\tilde{\mathbf{P}}_m = \nabla_{\boldsymbol{\theta}} \boldsymbol{\eta}_m = [\mathbf{P}_m, \mathbf{p}] \tag{25}$$

with $\mathbf{p} = [0, 1]^T$. Then the FIM concerning $\boldsymbol{\theta}$ will be

$$\mathbf{F}_{\boldsymbol{\theta}} = \sum_m \tilde{\mathbf{P}}_m^T \mathbf{F}_{\boldsymbol{\eta}_m} \tilde{\mathbf{P}}_m = \sum_m \begin{bmatrix} \mathbf{P}_m^T \mathbf{F}_{\boldsymbol{\eta}_m} \mathbf{P}_m & \mathbf{P}_m^T \mathbf{F}_{\boldsymbol{\eta}_m} \mathbf{p} \\ \mathbf{p}^T \mathbf{F}_{\boldsymbol{\eta}_m} \mathbf{P}_m & \mathbf{p}^T \mathbf{F}_{\boldsymbol{\eta}_m} \mathbf{p} \end{bmatrix}.$$

The CRLB of positioning error in this case will be

$$\tilde{\mathbf{R}}_\mathbf{x} = \mathbf{F}_{\boldsymbol{\theta}}^{-1}[1:2, 1;2] = \left(\mathbf{F}_\mathbf{x} - \mathbf{f}\mathbf{f}^T/p\right)^{-1} \tag{26}$$

with $\mathbf{f} = \sum_m \mathbf{P}_m^T \mathbf{F}_{\boldsymbol{\eta}_m} \mathbf{p}$, $p = \sum_m \mathbf{p}^T \mathbf{F}_{\boldsymbol{\eta}_m} \mathbf{p}$ and $\mathbf{F}_\mathbf{x}$ given in (22). Compared with the ToA-based approach, the TDoA-based localization will inevitably lose some information due to the non-synchronized clocks at transmitter and receiver, i.e., $\mathbf{R}_\mathbf{x} \leq \tilde{\mathbf{R}}_\mathbf{x}$.

Numerical results: In this part, we will numerically evaluate the previous analyses, by considering the scenario illustrated in Fig. 3. The target is constantly broadcasting a LFM signal, with initial frequency at $f_0 = 10$ kHz, $B = 400$ Hz, $k = 200$ Hz/s, and $T = 2$ s. The underwater sound speed is 1500 m/s. The AUV measures the Doppler shift, ToA and TDoA at three different positions, 20 meters away from each other. The distance between the center of these three positions to the target is denoted by $\bar{d}$.

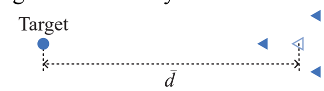

Fig. 3. Geometrical distribution of target and anchors.

In Fig. 4, the relation between positioning error and the condition number of the covariance matrix is presented. The first sub-figure shows the CRLB of positioning error of Doppler shift-based system. As we expected, when $\bar{d}$ increases, the positioning error will increase fast, mainly due to the increase of the condition number. For the ToA-based system in the second sub-figure, the positioning error grows proportionally with the square root of the condition number. The large condition number indicates that one eigenvalue of the FIM is particularly small. Suppose the FIM is $\mathbf{F}$, with two eigenvalues λ_0 and λ_1, and $\lambda_0 >> \lambda_1$. The CRLB of positioning error will be $1/\lambda_0 + 1/\lambda_1 \approx 1/\lambda_1$. That is, the variance of positioning error is mainly dependent on the smallest eigenvalue of the FIM. This also explains why the positioning error is proportional to the square root of the condition number. In the third and forth sub-figures, the positioning error will be significantly reduced when we combine the Doppler shift with ToA or TDoA measurements. The fundamental reason is that by combing two types of measurements, the smallest condition number of the FIM is significantly boosted. Their stronger sub-spaces (or eigenvalues) will strength the weak spots of each other, i.e., complementarity.

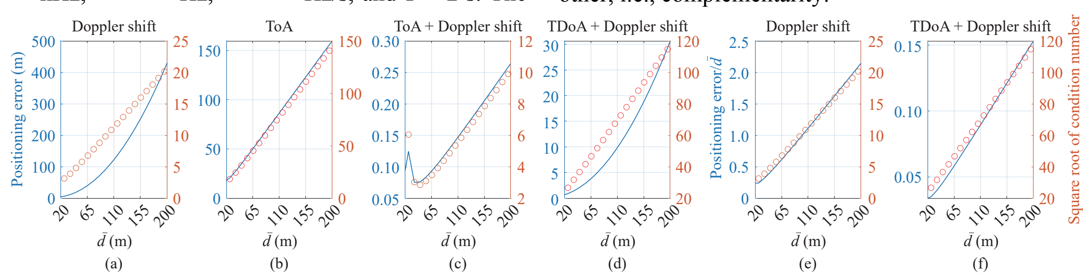

Fig. 4. Comparison of ToA-based, TDoA-based, and Doppler-based localization.

For Figs. 4(a) and 4(d), there seems to be another factor contributing to the positioning error, apart from the condition number. Based on our previous analysis, the factor is most probably the distance. To verify this, the positioning error for Doppler shift-based and TDoA-based systems normalized by $\bar{d}$ is presented in Figs. 4(e) and 4(f).

Conclusion: To summarize, we mathematically and qualitatively explained the challenges of far-field positioning based on one mobile anchor in underwater environments. Two reasons for the poor performance are unveiled: the long distance and the large condition number of the covariance matrix. They will amplify the measurement errors of Doppler shift, ToA and TDoA, etc. One possible solution is to combine different types of measurements for localization. By exploiting the diversity/complementarity of the measurements, we can significantly reduce the condition number, and thus reduce the positioning error. The huge potentials of such a strategy is demonstrated through the combination of Doppler shift with ToA or TDoA measurements, which can be done by employing LFM signals.

Acknowledgments: This work was supported by the National Natural Science Foundation of China (62201162), the HKUST(GZ) (Start-Up Founding, G0101000066), the Natural Sciences and Engineering Research Council (NSERC) of Canada (RGPIN-2018-03792), the IET SensorTECH (5404-2061-101), the Natural Science Foundation of Jiangsu Province (BK20190733), and the NUPTSF (NY219166).

References

[1] Z. Gong, C. Li, F. Jiang, and J. Zheng, "AUV-aided localization of underwater acoustic devices based on Doppler shift measurements," *IEEE Trans. Wireless Commun.*, vol. 19, no. 4, pp. 2226–2239, Apr. 2020.

[2] Q. Liang, B. Zhang, C. Zhao, and Y. Pi, "TDoA for passive localization: Underwater versus terrestrial environment," *IEEE Trans. Parallel Distributed Syst.*, vol. 24, no. 10, pp. 2100–2108, Oct. 2013.

[3] J. Zheng and Y. C. Wu, "Joint time synchronization and localization of an unknown node in wireless sensor networks," *IEEE Trans. Signal Processing*, vol. 58, no. 3, pp. 1309–1320, 2010.

[4] R. Diamant and L. Lampe, "Underwater localization with time-synchronization and propagation speed uncertainties," *IEEE Trans. Mobile Computing*, vol. 12, no. 7, pp. 1257–1269, Jul. 2013.

[5] S. Sun, X. Zhang, C. Zheng, J. Fu, and C. Zhao, "Underwater acoustical localization of the black box utilizing single autonomous underwater vehicle based on the second-order time difference of arrival," *IEEE J. Oceanic Engineering*, vol. 45, no. 4, Oct. 2020.

[6] Z. Gong, C. Li, and F. Jiang, "AUV-aided joint localization and time synchronization for underwater acoustic sensor networks," *IEEE Signal Processing Lett.*, vol. 25, no. 4, pp. 477–481, Apr. 2018.

[7] D. J. Peters, "A Bayesian method for localization by multistatic active sonar," *IEEE J. Oceanic Engineering*, vol. 42, no. 1, pp. 135–142, Jan. 2017.

[8] P. Carroll, K. Domrese, H. Zhou, S. Zhou, and P. Willett, "Doppler-aided localization of mobile nodes in an underwater distributed antenna system," *Physical Commun.*, vol. 18, pp. 49–59, Mar. 2016.

[9] M. M. Ahmed, K. C. Ho, and G. Wang, "Localization of a moving source by frequency measurements," *IEEE Trans. Signal Processing*, vol. 68, pp. 4839–4854, Aug. 2020.

[10] R. Spindel, R. Porter, W. Marquet, and J. Durham, "A high-resolution pulse-Doppler underwater acoustic navigation system," *IEEE J. Oceanic Engineering*, vol. 1, no. 1, pp. 6–13, Sept. 1976.

[11] J. Yan, X. Zhang, X. Luo, Y. Wang, C. Chen, and X. Guan, "Asynchronous localization with mobility prediction for underwater acoustic sensor networks," *IEEE Trans. Vehicular Technology*, vol. 67, no. 3, pp. 2543–2556, Mar. 2018.

[12] Y. Li, Y. Wang, W. Yu, and X. Guan, "Multiple autonomous underwater vehicle cooperative localization in anchor-free environments," *IEEE J. Oceanic Engineering*, vol. 44, no. 4, pp. 895–911, Oct. 2019.

[13] M. Erol, L. F. M. Vieira, and M. Gerla, "AUV-aided localization for underwater sensor networks," in *Proc. Int. Conf. Wireless Algorithms, Syst. and Applications,* Chicago, USA, Aug. 2007, pp. 44–54.